



# **The delayed recovery of the remobilized rat tibialis anterior muscle reflects a defect in proliferative and terminal differentiation that impairs early regenerative processes**

Lamia Slimani, Emilie Vazeille, Christiane Deval, Bruno Meunier, Cécile Polge, Dominique Dardevet, Daniel Bechet, Daniel Taillandier, Didier Micol, Anne Listrat, et al.

## **► To cite this version:**

Lamia Slimani, Emilie Vazeille, Christiane Deval, Bruno Meunier, Cécile Polge, et al.. The delayed recovery of the remobilized rat tibialis anterior muscle reflects a defect in proliferative and terminal differentiation that impairs early regenerative processes. *Journal of Cachexia, Sarcopenia and Muscle*, 2015, 6 (1), pp.73-83. 10.1002/jcsm.12011 . hal-01901485

**HAL Id: hal-01901485**

**<https://hal.science/hal-01901485>**

Submitted on 22 Oct 2018

**HAL** is a multi-disciplinary open access archive for the deposit and dissemination of scientific research documents, whether they are published or not. The documents may come from teaching and research institutions in France or abroad, or from public or private research centers.

L'archive ouverte pluridisciplinaire **HAL**, est destinée au dépôt et à la diffusion de documents scientifiques de niveau recherche, publiés ou non, émanant des établissements d'enseignement et de recherche français ou étrangers, des laboratoires publics ou privés.



Distributed under a Creative Commons Attribution - NonCommercial - NoDerivatives 4.0 International License

# The delayed recovery of the remobilized rat tibialis anterior muscle reflects a defect in proliferative and terminal differentiation that impairs early regenerative processes

Lamia Slimani<sup>1,2</sup>, Emilie Vazeille<sup>3</sup>, Christiane Deval<sup>1,2</sup>, Bruno Meunier<sup>4</sup>, Cécile Polge<sup>1,2</sup>, Dominique Dardevet<sup>1,2</sup>, Daniel Béchet<sup>1,2</sup>, Daniel Taillandier<sup>1,2</sup>, Didier Micol<sup>4</sup>, Anne Listrat<sup>4</sup>, Didier Attaix<sup>1,2</sup> & Lydie Combaret<sup>1,2\*</sup>

<sup>1</sup>INRA, UMR 1019, UNH, CRNH, F-63000 Auvergne, Clermont-Ferrand, France; <sup>2</sup>Clermont Université, Université d'Auvergne, Unité de Nutrition Humaine, BP 10448, F-63000 Clermont-Ferrand, France; <sup>3</sup>Centre Hospitalier Universitaire, 63000 Clermont-Ferrand, France; <sup>4</sup>INRA, UMR 1213 Herbivores, 63122 Saint Genès Champanelle, France

## Abstract

**Background** The immobilization-induced tibialis anterior (TA) muscle atrophy worsens after cast removal and is associated with altered extracellular matrix (ECM) composition. The secreted protein acidic and rich in cysteine (Sparc) is an ECM component involved in Akt activation and in  $\beta$ -catenin stabilization, which controls protein turnover and induces muscle regulatory factors (MRFs), respectively. We hypothesized that ECM alterations may influence these intracellular signalling pathways controlling TA muscle mass.

**Methods** Six-month-old Wistar rats were subjected to hindlimb cast immobilization for 8 days (I8) or not (I0) and allowed to recover for 1 to 10 days (R1–R10).

**Results** The TA atrophy during remobilization correlated with reduced fibre cross-sectional area and thickening of endomysium. mRNA levels for Sparc increased during remobilization until R10 and for integrin- $\alpha$ 7 and - $\beta$ 1 at I8 and R1. Integrin-linked kinase protein levels increased during immobilization and remobilization until R10. This was inversely correlated with changes in Akt phosphorylation.  $\beta$ -Catenin protein levels increased in the remobilized TA at R1 and R10. mRNA levels of the proliferative MRFs (Myf5 and MyoD) increased at I8 and R1, respectively, without changes in Myf5 protein levels. In contrast, myogenin mRNA levels (a terminal differentiation MRF) decreased at R1, but only increased at R10 in remobilized muscles, as for protein levels.

**Conclusions** Altogether, this suggests that the TA inefficiently attempted to preserve regeneration during immobilization by increasing transcription of proliferative MRFs, and that the TA could engage recovery during remobilization only when the terminal differentiation step of regeneration is enhanced.

**Keywords**  $\beta$ -Catenin; Extracellular matrix; Outside-In signaling; Recovery; Regeneration; Skeletal muscle atrophy

Received: 10 July 2014; Revised: 09 October 2014; Accepted: 15 October 2014

\*Correspondence to: Lydie Combaret, UMR 1019, Nutrition Humaine, Centre INRA, de Clermont-Ferrand/Theix, 63000 Clermont-Ferrand, France. Tel: +33(4)73624824, Fax: +33(4)73624755, Email: lydie.combaret@clermont.inra.fr

## Introduction

Skeletal muscle provides power and strength for locomotion and posture, but is also the major reservoir of body proteins that are mobilized during catabolic conditions to preserve vital functions. In contrast, sustained muscle wasting leads to weakening and severe metabolic consequences, which impact healthcare costs. Periods of immobilization or acute inactivity

in muscle-wasting conditions are associated with weakness and/or frailty, and this further contributes to muscle atrophy.

Muscle wasting results from an imbalance between protein synthesis and breakdown rates but also between apoptotic and regeneration processes.<sup>1–6</sup> These adaptations have been mostly investigated in the soleus and gastrocnemius muscles during disuse,<sup>7–20</sup> but are less clearly outlined during muscle recovery. We reported in previous studies that kinetics of muscle

recovery differed according to the muscle studied.<sup>5,3</sup> Actually, while the mass of the immobilized Gastrocnemius (GA) or soleus muscle stabilizes as soon as the cast is removed, the tibialis anterior (TA) muscle further atrophies, suggesting an important remodelling of that muscle.<sup>3,5</sup> These surprising observations deserve further attention: (1) indeed, the disused slow-twitch soleus muscle has been extensively studied but is not representative of the overall musculature, and consequently, (2) understanding the mechanisms involved in the fast-twitch TA and GA atrophy and recovery after immobilization should provide a more representative overview of muscle alterations.

We previously reported that changes in the structure (i.e. the thickening of connective tissue) and the composition (i.e. an increased remodelling of collagens) of the extracellular matrix (ECM) characterized the TA adaptations after cast removal,<sup>3</sup> suggesting that the ECM signalling to the myofibre, which controls muscle homeostasis, may have been impaired. The protein kinase Akt is involved in the control of protein turnover and, when inhibited, reduces protein synthesis and increases proteolysis.<sup>21</sup> Akt phosphorylation and activity was either unchanged<sup>22,23</sup> or reduced<sup>24</sup> after cast immobilization in rodent or human soleus and GA muscles. A single study reported that Akt phosphorylation increased rapidly in the recovering soleus after cast removal.<sup>24</sup> However, the regulation of Akt in the TA, which exhibits a particular pattern immediately after cast removal, is not documented. From the internal side of the myofibre, the Integrin-linked-kinase (Ilk) is a cytosolic partner of the transmembrane integrins,<sup>25,26</sup> which belong to ECM.<sup>27</sup> Ilk has been reported to be involved (i) in myogenesis in L6 muscle cells,<sup>28</sup> and (ii) in the control of Akt signalling in Hela cells,<sup>29,30</sup> but also *in vivo* in muscle.<sup>31</sup> Nevertheless, its kinase activity remained controversial.<sup>25,26,32</sup>

From the external side of the myofibre, the secreted protein acidic and rich in cysteine (Sparc) is a nonstructural, matricellular glycoprotein that is secreted into skeletal muscle progenitor cell niches. The Sparc has a role in cell adhesion, angiogenesis, and cell differentiation.<sup>33</sup> At the intracellular level, Sparc enhanced Ilk interaction with  $\beta$ 1-integrin heterodimers.<sup>30,34</sup> In addition, Sparc can induce the phosphorylation and activation of Akt in the presence of Ilk.<sup>30</sup> However, this was demonstrated in non-muscle cells. The loss of Sparc induced muscle atrophy and increased the expression of the muscle-specific E3 ubiquitin-ligase MAFbx/atrogen-1,<sup>33</sup> which seems presumably involved in the control of protein synthesis.<sup>35,36</sup> Regulation of myogenic differentiation by Sparc remained controversial. Indeed, Sparc was up-regulated during differentiation of C2C12 myoblasts.<sup>37</sup> Conversely, its overexpression abolished myogenic differentiation in these cells.<sup>33,38</sup> Sparc and Ilk have been reported to induce stabilization and nuclear translocation of  $\beta$ -catenin,<sup>39</sup> which is an essential mediator of myogenesis and muscle homeostasis. Indeed,  $\beta$ -catenin accumulation results in increased expression of the muscle regulatory factors (MRFs).<sup>40,41</sup> Altogether, these reports strongly support a role of both Ilk and Sparc in muscle regeneration that remains to be explored *in vivo*.

Thus, the aim of this study was to better understand the mechanisms responsible for the worsening of TA atrophy during remobilization by (i) investigating the regulation of Sparc and Ilk *in vivo* during immobilization and/or remobilization, and (ii) determining the effect on the Akt-dependent signalling and myogenic processes.

## Material and methods

### Animals and experimental design

The present study was approved by the Animal Care and Use Committee at the Institut National de la Recherche Agronomique (INRA) and adhered to the current legislation on animal experimentation in France. Male Wistar rats, 6 months old (Charles River Laboratories, L'Arbresle, France) were housed individually in controlled environmental conditions (room temperature 22°C; 12 h light–dark cycle, light period starting at 8 h), fed *ad libitum*, and given free access to water.<sup>5,4</sup>

After a 3 week adaptation period, rats were anaesthetized with forene inhalation and subjected to unilateral hindlimb immobilization via an Orfit-soft plaque (Gibaud). Rats were casted as described previously<sup>3–5</sup> so that TA muscles were immobilized in a lengthened position. Briefly, after 8 days of immobilization (I8,  $n=11$ ), casts were removed and animals ( $n=10–11$ ) were allowed to recover for one (R1), six (R6), and 10 (R10) days. A group of non-casted rats was also included and served as control (I0,  $n=11$ ). Because muscles may undergo ischemic processes during immobilization, we monitored animals daily to assess the possible occurrence of edema or inflammation. Casts were removed and changed whenever it was necessary. At the end of the immobilization period, less than 5% of the rats showed legs with redness, swelling, edema, or irritation, suggesting that casting did not induce significant blocking of blood flow. For convenience, muscles that were immobilized between I0 and I8 are named remobilized during the recovery period (R1–R10). At the end of the immobilization or recovery periods, animals were euthanized under pentobarbital sodium anaesthesia (50 mg/kg ip). TA skeletal muscles were carefully dissected, weighed, and frozen in liquid nitrogen. A central part of TA muscle was fixed at resting length using Tissue-Tek® OCT™ (Sakura Finetek, France), frozen in cooled isopentane (–100°C), and then stored at –80°C until histological analyses. The remaining part was finely pulverized in liquid nitrogen and stored at –80°C until further analyses.

### Histological analyses of muscles

Ten micrometer thick TA cross-sections were performed at –25°C using a cryostat (HM500M Microm International) and stained with Picro-Sirius red, which reveals intramuscular connective tissue (IMCT) in red.<sup>42</sup> Observations and image acquisitions were performed using a photonic microscope in

bright field mode (Olympus BX-51, Tokyo, Japan), coupled to a high-resolution cooled digital camera (Olympus DP72) and Cell-D software (Olympus Soft Imaging Solutions, Münster, Germany), as previously described.<sup>3</sup> Briefly, after image acquisition for each muscle section, image analysis was performed using the Visilog 6.9 software (Noesis, France). The green component of the initial image was used for higher contrast, and top-hat filtering followed by manual thresholding on grey level allowed segmentation of the connective tissue network (perimysium and endomysium). Measurement of the area of this network was performed by counting the number of pixels in the resulting binary images and was expressed in percentage of the total field area. Additional segmentation of the connective network using the watershed algorithm results in separating objects corresponding to muscle cells.<sup>3</sup> Fibre boundaries were manually corrected when necessary.

### RNA extraction and real-time PCR

Total RNA was extracted from TA samples using TRIzol reagent (Invitrogen) according to the manufacturer's instructions. RNA concentration was determined with a Nanodrop ND 1000 spectrophotometer, and the integrity of the RNA was evaluated with a bioanalyzer (Agilent Technologies). One microgram of RNA was treated with DNase I Amp grade (Invitrogen), prior to cDNA Synthesis. Treated RNA was reverse transcribed using random primers and superscript II reverse transcription kit (Invitrogen) according to the manufacturer instructions. Real-time PCR was carried out using the CFX96 Real-time PCR detection system (Biorad). PCR reactions were performed using the IQ SYBR Green Supermix (Bio-Rad) according to the manufacturer's instructions. The primer sequences used are given in Table 1. The comparative threshold cycle ( $2^{-\Delta\Delta CT}$ ) method,<sup>43</sup> with 18S rRNA as a reference gene, was used to compare the relative mRNA expression between each group, where the relative mRNA abundance was arbitrarily set to one for IO group.

### Protein content measurements

One hundred milligrams of TA muscle powder from contralateral control and immobilized hindlimbs at each time point were homogenized using a polytron in 10 volumes of an ice-cold

buffer that was freshly prepared (pH 7.4) [20 mM Hepes, 50 mM  $\beta$ -glycerophosphate, 100 mM potassium chloride, 50 mM sodium fluoride, 2 mM EGTA, 0.2 mM EDTA, 1 mM dithiothreitol (DTT), 1 mM benzamidine, 0.5 mM sodium vanadate, 1% triton X100, 0.1 mM phenylmethylsulfonyl fluoride (PMSF), and proteinase inhibitor cocktail (Sigma, France)]. Homogenates were centrifuged at 14 500 g for 12 min at 4°C. The protein content was determined according to the Bio-Rad Protein Assay kit. Aliquots of supernatants were diluted in Laemmli sample buffer and stored at -80°C until use. Protein contents for Akt, Ilk,  $\beta$ -catenin, MyoG, and Myf5 were assessed by immunoblotting. Briefly, equal amounts of proteins were separated by Sodium Dodecyl Sulfate-PolyAcrylamide Gel Electrophoresis (SDS-PAGE) on 10% acrylamide gels, and transferred onto a PVDF membrane (Hybond P, Amersham). For Ilk,  $\beta$ -catenin, MyoG, and Myf5 immunodetection, blots were blocked for 1 h at room temperature with 5% skim milk in 1X TBST (15 mM Tris, 137 mM NaCl, 0.1% Tween20, and pH 7.8). For total Akt and phospho-Akt (Ser473) immunodetection, blots were blocked with 5% Bovine Serum Albumine (BSA). Then, blots were washed thrice in 1X TBST and incubated with the primary antibody diluted in 5% BSA in 1X TBST (overnight, stirring, 4°C). Anti-Ilk, anti- $\beta$ -catenin, and anti-MyoG (Sigma-Aldrich, Lyon, France) were respectively used at 1/5000, 1/10 000, and 1/1000 dilutions. Anti-total Akt and anti-Phospho-Akt (Ser473) (Cell Signaling Technology, Danvers, MA, USA) were used at 1/5000 and 1/2000 dilutions, respectively. Anti-Myf5 (Santa Cruz Biotechnology, Dallas, TX, USA) was used at 1/500 dilution. Blots were then washed thrice in 1X TBST and incubated with an appropriate secondary horseradish peroxidase conjugated antibody for 1 h at room temperature. Detection was performed using the Luminata Forte Western HRP substrate (Millipore) after washing the blots three times in 1X TBST. For all immunoblots, chemiluminescence was visualized using the G: BOX ChemiXT4 (XL1) (Syngene). Signals were then quantified using the GeneTools software (Syngene) and normalized against the amount of proteins in each lane (determined following Ponceau red staining) to correct for uneven loading.

### Statistical analysis

Statistical analyses were performed using Statistical Analysis Systems 9.1 procedures (SAS Institute Inc., Cary, NC, USA).

**Table 1** Primers used for quantitative Reverse Transcription-PCR analysis

Primer names	Accession number	Primer sense sequences	Primer antisense sequences
$\beta$ -catenin	NM_053357	5'-CGGATTGTGATCCGAGGACT-3'	5'-ACAGAGGACCCCTGCAGCTA-3'
Ilk	NM_133409	5'-GCACGCACTCAATAGCCGTA-3'	5'-ACCCAGGACAGGTGCATACAT-3'
Myod1	NM_176079	5'-CTGCTCTGATGGCATGATGG-3'	5'-ACTGTAGTAGGCGGCGTCGT-3'
Myf5	NM_001106783	5'-TGTCTGGTCCCGAAAGAACA-3'	5'-CAAGCAATCCAAGCTGGACA-3'
MyoG	NM_017115	5'-TCCCAACCCAGGAGATCATT-3'	5'-TATCCTCCACCGTGATGCTG-3'
Sparc	NM_12656	5'-TGGACTACATCGGACCATGC-3'	5'-TGACCAGGACGTTTTTGAGC-3'
18S rRNA	NR_046237	5'-AATCAGTTATGGTTCCTTTGTCG-3'	5'-GCTCTAGAATTACCACAGTTATCCAA-3'

Ilk, Integrin-linked kinase; Myf5, Myogenic factor 5; Sparc, Secreted protein acidic and rich in cysteine; MyoG, Myogenin.

Data were analysed for normality and equal variances. No set of data was transformed for non-normality distribution. Data were analysed by two-way analysis of variance for the effects of immobilization and stage of immobilization recovery and their interactions. In these analyses, an animal effect (paired effect), nested within the stage of immobilization-recovery, was introduced to take into account the fact that the Control and Immobilized muscles were sampled from the same animal. Multiple comparisons of adjusted means were based on Tukey's test. Level of significance was set at  $P \leq 0.05$ .

## Results

### *Tibialis anterior muscle atrophy is associated with reduced fibre cross-sectional area (CSA) and thickening of endomysium and perimysium*

The atrophy of immobilized TA muscles at I8 (18%,  $P < 0.05$  vs. I0) worsened between R1 and R10 (22%, 35%, and 24% at R1, R6, and R10, respectively,  $P < 0.05$  vs. I0) (Table 2). The contralateral non-immobilized muscle mass slightly decreased at I8 and R1 by 11% and 9%, respectively ( $P < 0.05$  vs. I0). Structural muscle alterations during immobilization and/or recovery were assessed after Sirius Red coloration to determine (i) muscle fibre cross-sectional area and (ii) endomysium (i.e. sheathing each individual muscle fibre) and perimysium (i.e. grouping muscle fibres into fascicles) areas.

Muscle fibre CSA from immobilized TA decreased from I8 (−28%,  $P < 0.05$ ) until R10 (−33%,  $P < 0.05$ ) when compared with I0 (Figure 1(A)–(B)). As observed for muscle mass, the contralateral non-immobilized muscle also exhibited a slight diminution of muscle fibre CSA from I8 until R6 (−15%,  $P < 0.05$  vs. I0) (Figure 1(A)–(B)). The perimysium area increased in the immobilized TA at I8 (+39%,  $P < 0.05$  vs. I0) and remained elevated in the remobilized muscles until R10 (+30%,  $P < 0.05$  vs. I0), except for R1 (Figure 1(A) and (C)).

**Table 2** Tibialis muscle mass following immobilization and remobilization

Stage	CTL (g)	IMM (g)
I0	0.796 ± 0.018	0.796 ± 0.018
I8	0.708 ± 0.022 <sup>§</sup>	0.656 ± 0.014 <sup>§</sup>
R1	0.725 ± 0.018 <sup>§</sup>	0.619 ± 0.023 <sup>*§</sup>
R6	0.769 ± 0.026	0.519 ± 0.021 <sup>*§</sup>
R10	0.824 ± 0.024	0.604 ± 0.020 <sup>*§</sup>

Values are means ± SE for  $n = 10$ –11 rats. CTL, control contralateral tibialis anterior; IMM, immobilized tibialis anterior. I0, before hindlimb casting; I8, immobilized for 8 days; R1–R10, remobilized for 1–10 days. Differences from CTL or I0 were assessed by analysis of variance.

\* $P < 0.05$  vs. CTL.

§ $P < 0.05$  vs. I0.

Meanwhile, the endomysium area did not change in the immobilized TA at I8, but increased in remobilized muscles from R1 to R10 (+20 to 39%,  $P < 0.05$  vs. I0) (Figure 1(A) and (C)). A further additional thickening of the endomysium occurred at R6 and R10 (+13% and 15%, respectively,  $P < 0.05$  vs. R1) (Figure 1(A) and (C)). Thus, the worsening of TA muscle atrophy during remobilization mainly correlated with a thickening of the endomysium area.

### *mRNA levels for Sparc, Integrin- $\alpha$ 7 and - $\beta$ 1 increased in the immobilized and/or remobilized TA*

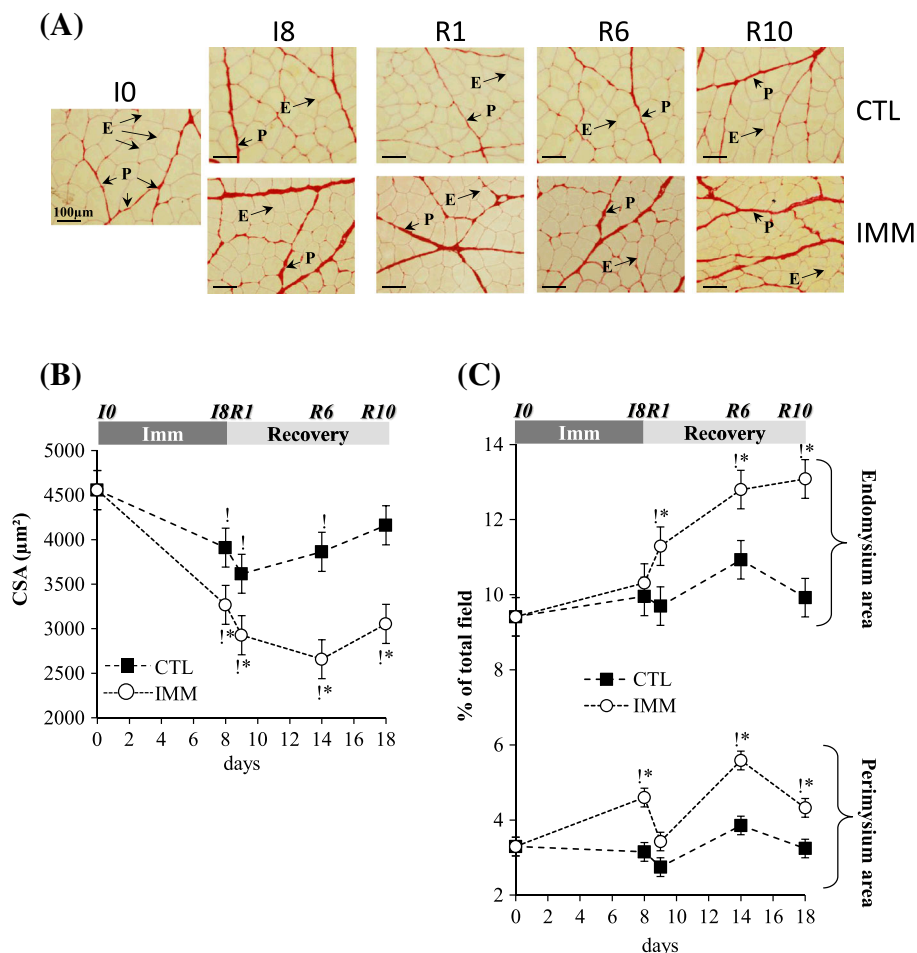
We then aimed at characterizing the regulation of the matricellular protein Sparc, which is involved in remodelling of damaged tissues.<sup>37</sup> Figure 2(A) shows that mRNA levels for Sparc did not change in the immobilized TA at I8, but strongly increased in the remobilized TA at R1 and R10 (+115% and +158%,  $P < 0.05$  vs. I8). In addition to its role in muscle regeneration, Sparc was suggested to bind to integrins (Itgs) in different cell types.<sup>23,34</sup> We show here that mRNA levels for Itg- $\alpha$ 7 and - $\beta$ 1 increased in the immobilized TA at I8 (+218% and 93%, respectively,  $P < 0.05$  vs. I0) and in the remobilized TA at R1 (+192% and 95%, respectively,  $P < 0.05$  vs. I0), before being normalized at R6 (Figure 2(B) and (C)). Altogether, this suggests that ECM structural alterations (Figure 1) during immobilization and remobilization were accompanied with changes in the ECM composition that may alter the outside-in signal transduction.

### *Increased integrin-linked kinase protein levels in TA muscle during immobilization and remobilization are inversely correlated to changes in Akt phosphorylation*

Sparc and Ilk were reported to induce the serine 473 phosphorylation of the protein kinase Akt.<sup>32,26</sup> We thus investigated the regulation of Ilk and Akt in the TA during immobilization and remobilization. Protein levels of Ilk increased in the immobilized TA at I8 (+83%,  $P < 0.05$  vs. I0), remained stable in the remobilized TA at R1, and then further increased at R6 until R10 (+~150%,  $P < 0.05$  vs. I0) (Figure 3(A) and (B)). Akt phosphorylation was assessed by measuring protein contents for total and serine 473 phosphorylated Akt (Figure 3(A)). The P-Ser473Akt/Akt ratio decreased in the immobilized TA at I8 and in the remobilized TA at R1 by 40% and 56%, respectively ( $P < 0.05$  vs. I0), and was normalized at R6 (Figure 3(A) and (C)). The P-Ser473Akt/Akt ratio slightly decreased at R1 in the contralateral TA compared with I0 (12%,  $P < 0.05$ ). Overall, and surprisingly, changes in Ilk protein levels, like those of Sparc mRNA, in the immobilized and remobilized TA inversely correlated with changes in the P-Ser473Akt/Akt ratio.



**Figure 1** Tibialis anterior muscle atrophy and extracellular matrix structural alterations during immobilization and remobilization. Tibialis anterior muscle sections were stained for fibre and extracellular matrix areas with Sirius Red. Image analysis of fibre cross-sectional area (A–B) and endomysium and perimysium areas (A–C) from immobilized and contralateral control muscles was performed as described in Methods. Values are means  $\pm$  SE (vertical bars) for  $n=8$  rats per group. Statistical differences were assessed by analysis of variance. \*,  $P<0.05$  vs. contralateral tibialis anterior;  $P<0.05$  vs. I0; I8, 8 days of hindlimb immobilization; R1–R10, remobilized for 1–10 days.

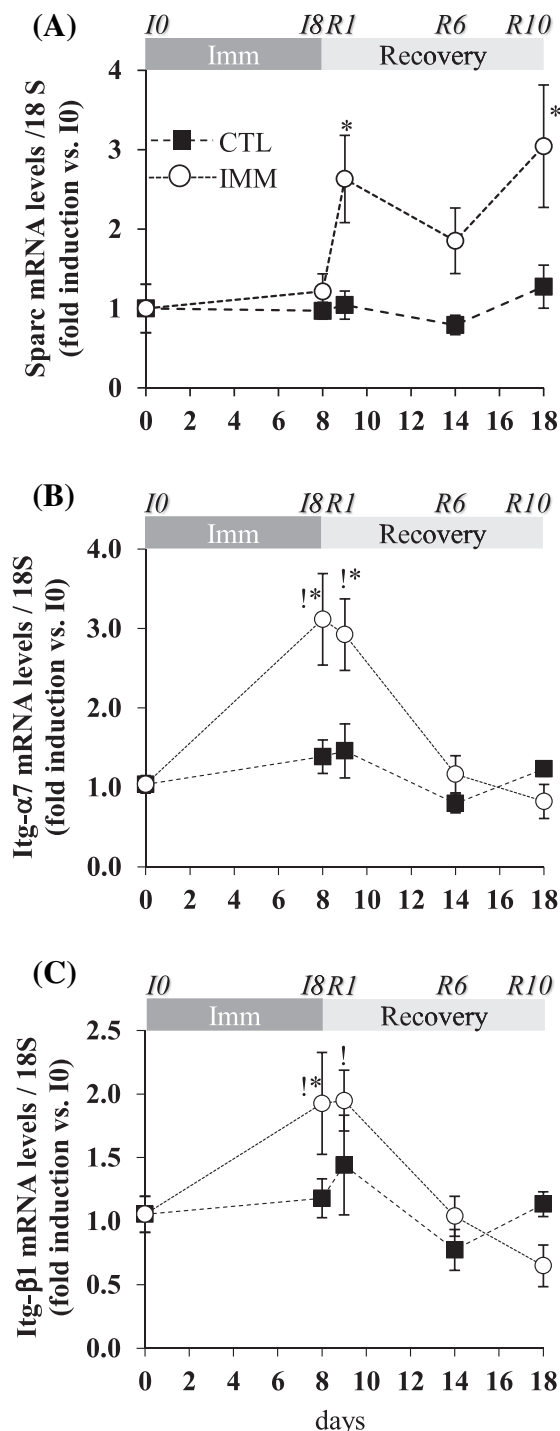


### Stabilization of $\beta$ -catenin in TA muscle during immobilization and/or recovery is associated with temporal regulation of MRFs expression

To better understand the significance of the induction of Sparc and Ilk mRNA or protein levels immediately after remobilization, we investigated the regulation of regeneration processes. Sparc and Ilk are also involved in the stabilization of  $\beta$ -catenin,<sup>39</sup> which is involved in MRFs transcription.<sup>31</sup>  $\beta$ -Catenin protein levels tended to be elevated in the immobilized TA at I8 (+50%,  $P>0.05$  vs. contralateral TA) (Figure 4(A) and (B)). In contrast,  $\beta$ -catenin protein levels dramatically increased in the remobilized TA at R1 (+220% and +345%,  $P<0.05$  vs. contralateral TA and I0 respectively) remained elevated but to a lesser extent at R6 (+141%,  $P<0.05$  vs. I0) and then increased again at R10 (+375% and +100%,  $P<0.05$  vs. I0 and remobilized TA at R6,

respectively) (Figure 4(A) and (B)). mRNAs encoding the first synthesized MRFs MyoD and Myf5 increased in the immobilized TA at I8 (+153% and 820%,  $P<0.05$  vs. I0, respectively) and remained elevated in the remobilized TA at R1 (+175% and 565%,  $P<0.05$  vs. I0, respectively), before being normalized at R6 (Figure 4(C) and (D)). This was not associated with changes in Myf5 protein levels during immobilization or remobilization (Figure 4(F)). Conversely, mRNA levels for the terminal differentiation MRF myogenin (MyoG) tended to decrease in the immobilized TA at I8 (−57% and −72%,  $P>0.05$  vs. contralateral TA and I0, respectively) (Figure 4(E)). In the remobilized TA, mRNA levels of MyoG were dramatically reduced at R1 (by 93%,  $P<0.05$  vs. contralateral TA or I0), but then progressively increased until R10 (+120% and 93%,  $P<0.05$  vs. contralateral TA and I0, respectively) (Figure 4(E)). MyoG protein levels did not change at I8 and R1, but increased at R6 (+43% and 12%,  $P<0.05$  vs. I0 and

**Figure 2** The secreted protein acidic and rich in cysteine (Sparc) and integrin (Itg) mRNA levels in the immobilized and remobilized tibialis anterior. mRNA levels for Sparc (A), Itg- $\alpha 7$  (B), and - $\beta 1$  (C) were measured by RT-qPCR in immobilized and contralateral control tibialis anterior muscles. Data were normalized using 18S rRNA and expressed as fold induction compared with I0 group. Data are means  $\pm$  SE (vertical bars) for  $n = 4$ –5 rats per group. Statistical differences were assessed by analysis of variance. \*,  $P < 0.05$  vs. contralateral tibialis anterior; !,  $P < 0.05$  vs. I0; I8, 8 days of hindlimb immobilization; R1–R10, remobilized for 1–10 days.



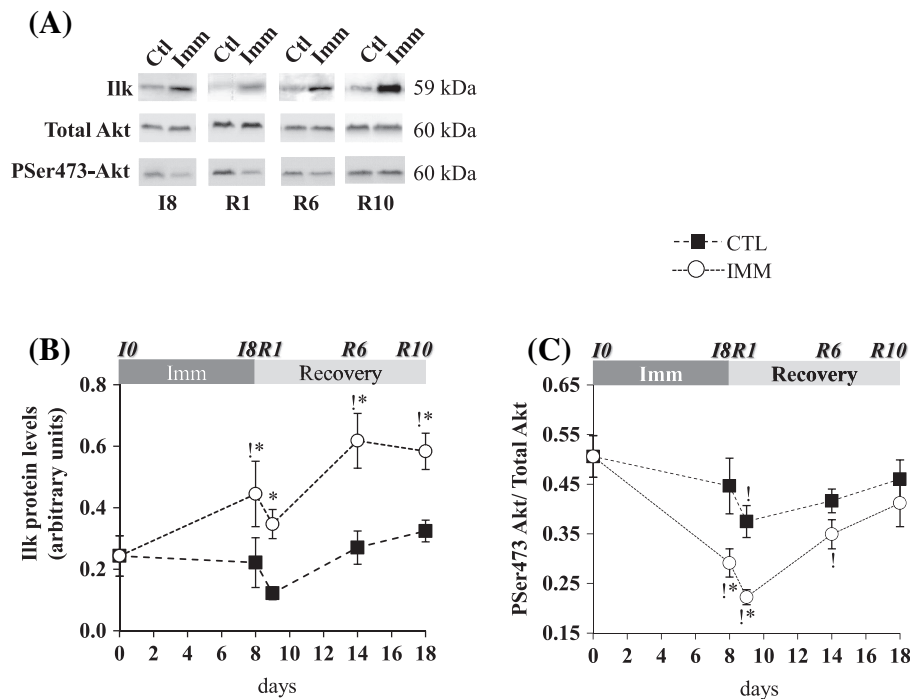
contralateral TA) and R10 (+63% and 42%,  $P < 0.05$  vs. I0 and contralateral TA) (Figure 4(G)). Thus,  $\beta$ -catenin protein levels were elevated in immobilized and remobilized TA, concomitantly with the induction of MyoD and Myf5 during immobilization and of MyoG later on during remobilization.

## Discussion

We report here that (i) the thickening of IMCT reflected alterations in both perimysium and endomysium areas. We also show that (ii) Sparc mRNA and Ilk protein levels were significantly induced in the remobilized TA immediately after cast removal, concomitantly with a major elevation of  $\beta$ -catenin protein levels, but without increasing the phosphorylation of Akt. Finally, (iii)  $\beta$ -catenin protein levels followed a wave-like kinetic, where the protein level increase was extremely important at R1 and R10 in the remobilized TA and modest at R6. This correlates with increased mRNA levels for Myf5 and MyoD at I8, which were then normalized at R6 and with higher mRNA levels for MyoG at only R10.

In agreement with the increase in connective tissue, which was parallel to the loss of contractile mass, we report here that muscle fibre CSA decreased during immobilization and remained low during remobilization in the TA. These changes occurred simultaneously with the decrease of TA muscle mass during immobilization and remobilization. A small decrease in muscle fibre CSA was also observed in the contralateral TA, without changes in muscle weight. This may result from a general decrease in the activity level of the animals, although immobilization was applied unilaterally. After cast removal, animals regained general activity concomitantly with the progressive normalization of the muscle fibre CSA of the contralateral TA. We previously showed a possible fast-to-slow change in metabolic properties of the remobilized TA,<sup>3</sup> which was also reported in the TA muscle of tetra/paraplegic patients when its usage is significantly increased.<sup>44</sup> However, in the latter study, these changes prevailed at the mRNA levels of Myosin Heavy Chain isoforms only after 4–9 weeks of electrical stimulation, without changes in protein levels, whose modifications are likely delayed.<sup>44</sup> Altogether, this suggests that the response of TA muscle to immobilization and remobilization may be delayed, thus impairing the recovery/regeneration abilities of this muscle. Immobilizing muscle in a lengthened position may constitute a hypertrophic stimulus with increased MyoG and IGF1 expression.<sup>45,46</sup> However, we report here that immobilization of the TA did not result in hypertrophy but in atrophy resulting from increased proteolysis<sup>3</sup> and presumably from depressed protein synthesis as suggested by the reduction in Akt phosphorylation (Figure 3). Thus, our model of immobilization did not correlate with changes reported in studies that focused on stretch stimulus, since we also observed either a decrease or no change in MyoG mRNA or protein levels, respectively.

**Figure 3** Ilk mRNA and protein levels and Akt phosphorylation in immobilized and remobilized tibialis anterior. (A) Protein levels for Ilk, Akt, and P-Ser473-Akt were assessed by Western blots. Representative Western blots are shown, and noncontiguous gel lanes are demarcated by white spaces. After quantification, Ilk protein signals were normalized using Ponceau red staining for uneven loading (B), and the ratio P-Ser<sub>473</sub>Akt / Total Akt (C) was calculated. Statistical differences were assessed by analysis of variance. \*,  $P < 0.05$  vs. contralateral tibialis anterior; †,  $P < 0.05$  vs. I0; I8, 8 days of hindlimb immobilization; R1–R10, remobilized for 1–10 days.



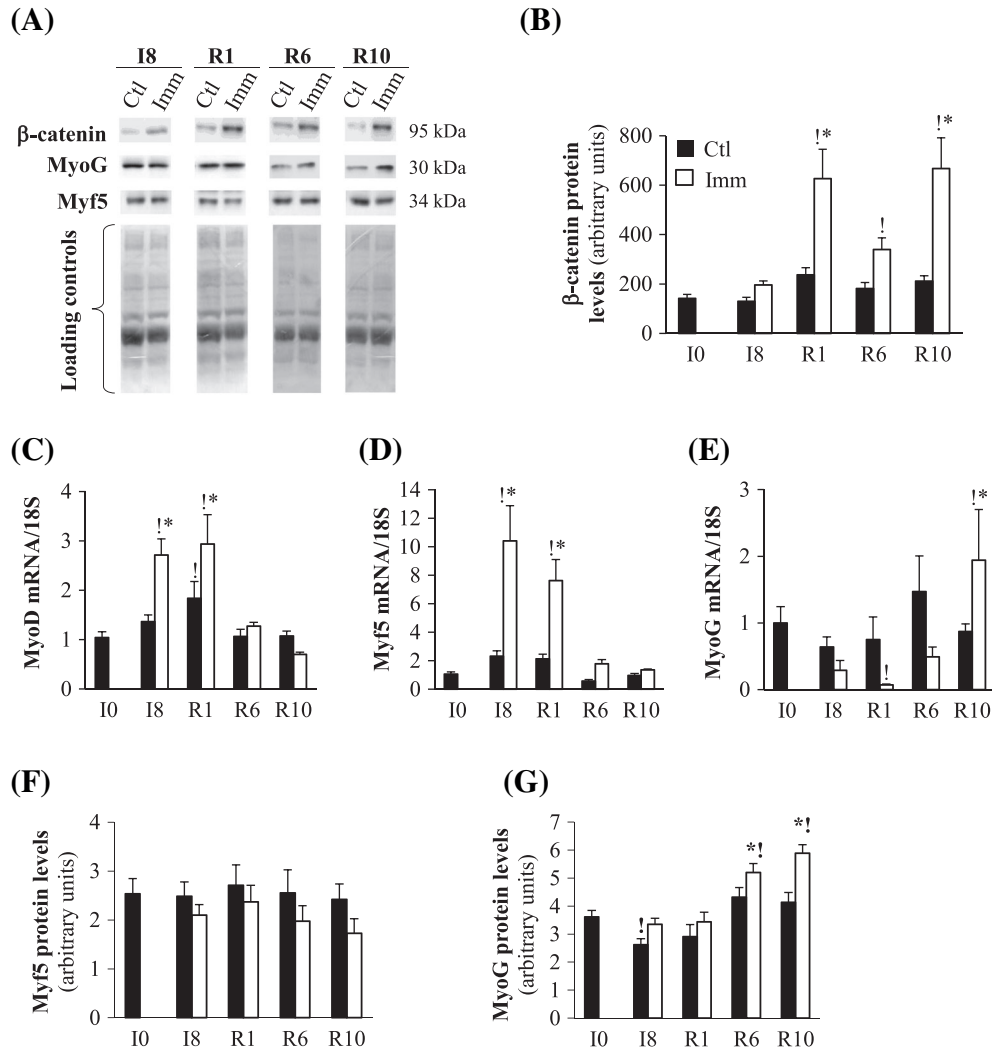
We also report an increase in the perimysium area during immobilization, but of the endomysium area during remobilization. This suggests a remodelling that cannot solely reflect the reduction in muscle fibre CSA. However, we cannot exclude that the area of endomysium and/or perimysium may have been under- and/or over-estimated. Indeed, (i) the IMCT reflects a continuum of endomysium and perimysium from one muscle myofibre to another, and (ii) the estimation of endomysium and perimysium areas is based on a threshold on a grey level for the segmentation of the connective tissue network. The reported ECM adaptations may, however, impact muscle function by (i) influencing shear strain accommodation during muscle contraction and extension<sup>47</sup> and/or (ii) delaying recovery because of defects in tensile force transmission after remobilization.<sup>48</sup> Our findings indicating that the endomysium area did not change during immobilization agreed with a geometrical model predicting that changing the length of muscle fibre is not affecting endomysium thickness.<sup>49</sup> When remobilized, the TA moved rapidly from a lengthened to a shortened position, which may result in the thickening observed. In addition, the acute shortening of the TA may also constitute an atrophic stimulus responsible for the additional muscle wasting that prevailed during remobilization. Between I8 and R1 (i.e. immediately after cast removal), the perimysium area was reduced while the

endomysium area increased. We previously reported that although the expression of the major fibrillar collagen 1 increased dramatically between I8 and R1, suggesting collagen deposition, the global IMCT area did not change between I8 and R1 in the remobilized TA, but later on at R6 and R10.<sup>3</sup> These data suggest that an adaptive response to sudden forces is experienced by the TA when stretching was released upon cast removal that may result in a redistribution and/or reorientation of fibre bundles and thus in changes of the continuum between endomysium and perimysium. Altogether, our data indicate that the worsening of TA muscle atrophy during remobilization was associated with pronounced changes in the structure and the composition of muscle fibres and ECM.

We report here that these ECM structural alterations were associated with increased expression of Sparc, Itg- $\alpha 7$  and  $\beta 1$ , and Ilk during either immobilization or remobilization. This suggests that alterations in the ECM composition may impact signal transduction to muscle cells. In fact, Sparc induced phosphorylation of Akt in an Ilk-dependent manner in glioma cells.<sup>30</sup> Ilk seems to be involved in Akt phosphorylation, although its role remains controversial as to whether or not this is a direct effect.<sup>26,29,30,32</sup> In this study, however, the increased expression of Ilk and Sparc in either the immobilized and/or the remobilized TA did not correlate with



**Figure 4**  $\beta$ -Catenin stability and myogenic factor mRNA and protein levels in immobilized and remobilized tibialis anterior. Protein levels for  $\beta$ -catenin (A, B), Myf5 (A, F), and MyoG (A, G) were assessed in the immobilized and contralateral control tibialis anterior by Western blots (A), quantified and normalized using Ponceau red staining for uneven loading as described in Materials and Methods. Representative Western blots are shown and noncontiguous gel lanes are demarcated by white spaces (A). mRNA levels for MyoD (C), Myf-5 (D) and Myogenin (MyoG) (E) were assessed by RT-qPCR, normalized using 18S rRNA and expressed as fold induction compared with I0 group. Data are means  $\pm$  SE for  $n=4-8$  rats per group. Statistical differences were assessed by analysis of variance. \*,  $P < 0.05$  vs. contralateral tibialis anterior; !,  $P < 0.05$  vs. I0; I8, 8 days of hindlimb immobilization; R1–R10, remobilized for 1–10 days.



an increase in Akt phosphorylation, but rather with a decrease in P-Ser473Akt/Akt ratio. In addition, Akt phosphorylation also slightly decreased in the contralateral TA immediately during the immobilization period, presumably due to a general decrease in the activity level of the animals. Nevertheless, animals resumed utilizing their previously immobilized leg within 2–3 days of remobilization, and this is in agreement with the normalization of the P-Ser473Akt/Akt ratio in the contralateral leg at R6.

Most studies on muscle wasting and recovery were performed in the gastrocnemius or soleus muscle, which atrophy substantially during muscle inactivity.<sup>3,5</sup> In these studies,

muscle loss stopped as soon as the cast was removed and proteolysis returned quite rapidly to basal values. However, this is not the case for all muscles, such as the TA, which atrophied also after remobilization owing to a sustained activation of muscle proteolysis.<sup>3</sup> A decrease in Akt phosphorylation induces the nuclear translocation of the transcription factor FoxO3 and, thus, the transcription of genes involved in the ubiquitin-proteasome-dependent proteolysis (UPS).<sup>50</sup> Thus, the decreased Akt phosphorylation in both the immobilized and remobilized TA reported here is in accordance with the sustained activation of the UPS.<sup>3</sup> However, we also reported here that Sparc and Ilk, which have been

shown to induce Akt phosphorylation,<sup>29–31</sup> were up-regulated in the remobilized TA concomitantly with the reduced Akt phosphorylation. Altogether, our data indicate that the activation of muscle proteolysis and the inactivation of the Akt-dependent signalling in the immobilized and remobilized TA are independent of Sparc and Ilk. Nevertheless, we report here for the first time that mRNA levels for the matricellular protein Sparc and protein levels of Ilk increased immediately after remobilization in the TA muscle.

Our data differ from the observation that the suppression of Sparc in TA muscles led to myofibre atrophy and increased expression of the muscle-specific E3 ligase MAFbx/Atrogin-1.<sup>33</sup> However, Sparc may also play a role in muscle atrophy and recovery after immobilization through alternative pathways, such as regeneration processes. Ilk and Sparc are involved in  $\beta$ -catenin stabilization<sup>33,39</sup> and in the control of MRF transcription.<sup>31,37</sup> The increased Sparc and Ilk expression (see Figure 2 and 3, respectively) immediately after cast removal suggests that regeneration processes were early initiated to favour muscle repair in the remobilized TA. Consistently,  $\beta$ -catenin protein levels were elevated at R1, concomitantly with sustained increases in Myf5 and MyoD mRNA levels. However, protein levels of the proliferative MRF Myf5 did not change, suggesting that the immobilized TA inefficiently attempted to preserve regeneration during immobilization, presumably contributing to muscle atrophy. MyoG mRNA levels dramatically decreased early after cast removal, with no change in protein levels. We also report here that MyoG mRNA and protein levels increased between R6 and R10 when muscle atrophy stopped. The relationships between Sparc, Ilk, and regeneration processes are complex. Actually, Sparc inhibited the differentiation processes in C2C12 myotubes,<sup>33,38</sup> whereas Ilk was a positive mediator of L6 myoblast differentiation.<sup>28</sup> By decreasing the expression of MyoD, Myf5, and MyoG in C2C12 cells, Sparc should have a global negative effect on myogenesis.<sup>38</sup> This is different from our data, which show that Sparc overexpression during remobilization correlated with an increase in MyoD and Myf5 expression. However, the substantial decrease in MyoG mRNA levels is in agreement with a negative role of Sparc on muscle cell differentiation.<sup>33,38</sup> The overexpression of MyoD and Myf5 may result from the regulation of other signalling cascades. Ilk has also been reported to repress the initiation of terminal myogenic differentiation, in accordance with the down regulation of MyoG seen here, but to be required for normal morphogenesis of myotubes.<sup>51</sup> This suggests that Ilk functions not only in the initial orientating process, but also in later stages (fusion or maintaining myotube integrity) of myogenic differentiation. Altogether, our data suggest that induction of Sparc and Ilk may stabilize  $\beta$ -catenin, increasing transcription of MyoD and Myf5 and without any positive effect on TA recovery during remobilization, since

the final differentiation step was repressed, as presumably indicated by the decreased mRNA for MyoG. The regulation of satellite cell activation, proliferation, and differentiation is complex, and thus, we cannot exclude that activation and/or proliferation of these cells was also impaired although MyoD and Myf5 mRNA levels increased. However, the activation of the Sparc-Ilk- $\beta$ -catenin signalling pathway may contribute to muscle recovery at R10, when MyoG mRNA and protein increased (Figure 4(D)). In addition, the data show that although mRNA levels for Myf5 and MyoD were up-regulated, protein levels did not change. This suggests that cells are regulating these early MRFs at the post-transcriptional level.

In conclusion, we show that remobilization of immobilized TA muscle induced deep changes in the structure and composition of the ECM and in intracellular signalling pathways involved in muscle regeneration. Indeed, muscle recovery takes place slowly in the remobilized TA. This is consistent with a scheme where muscle cells attempted to develop an appropriated potential regeneration process through increasing proliferative MRFs transcription, possibly controlled by Sparc and Ilk induction and  $\beta$ -catenin stabilization. However, our data suggest that this process was poorly efficient at the early stages of remobilization, presumably owing to an alteration of the post-transcriptional regulation of proliferative MRFs and of the final differentiation step of regeneration.

## Acknowledgements

We thank Arlette Cissoire, Benoit Cohade, and Philippe Lhoste from the UEN (INRA Clermont-Ferrand-Theix, France) for excellent assistance with animal care. We are grateful to Agnès Claustre, Cécile Coudy, and Marianne Jarzaguet for their help during animal slaughtering, sample care, and technical assistance. We also thank Julien Amat, Isabelle Cassar-Malek, Geoffrey Delcros, Jean-Yves Exposito, and Geneviève Gentes for RT-qPCR measurements. This study was supported by grants from the Institut National de la Recherche Agronomique, the Association Française contre les Myopathies, and the Société Française de Nutrition. LS was supported by a PhD fellowship from the Ministère de l'Enseignement Supérieur et de la Recherche. The authors certify that they comply with the ethical guidelines for authorship and publishing of the Journal of Cachexia, Sarcopenia and Muscle (von Haehling S, Morley JE, Coats AJS, Anker SD. Ethical guidelines for authorship and publishing in the Journal of Cachexia, Sarcopenia and Muscle. J Cachexia Sarcopenia Muscle 2010;1:7–8).

## Conflict of interest

None declared.

## References

- Evans WJ. Skeletal muscle loss: cachexia, sarcopenia, and inactivity. *Am J Clin Nutr* 2010; **91**: 1123S–1127S.
- Magne H, Savary-Auzeloux I, Vazeille E, Claustre A, Attaix D, Lestrat A, Veronique SL, Philippe G, Dardevet D, Combaret L. Lack of muscle recovery after immobilization in old rats does not result from a defect in normalization of the ubiquitin-proteasome and the caspase-dependent apoptotic pathways. *J Physiol* 2011; **589**: 511–524. doi:10.1113/jphysiol.2010.201707.
- Slimani L, Micol D, Amat J, Delcros G, Meunier B, Taillandier D, Polge C, Bechet D, Dardevet D, Picard B, Attaix D, Lestrat A, Combaret L. The worsening of tibialis anterior muscle atrophy during recovery post-immobilization correlates with enhanced connective tissue area, proteolysis, and apoptosis. *Am J Physiol Endocrinol Metab* 2012; **303**: E1335–E1347. doi:10.1152/ajpendo.00379.2012.
- Vazeille E, Slimani L, Claustre A, Magne H, Labas R, Bechet D, Taillandier D, Dardevet D, Astruc T, Attaix D, Combaret L. Curcumin treatment prevents increased proteasome and apoptosome activities in rat skeletal muscle during reloading and improves subsequent recovery. *J Nutr Biochem* 2012; **23**: 245–251. doi:10.1016/j.jnutbio.2010.11.021.
- Vazeille E, Codran A, Claustre A, Averous J, Lestrat A, Bechet D, Taillandier D, Dardevet D, Astruc T, Attaix D, Combaret L. The ubiquitin-proteasome and the mitochondria-associated apoptotic pathways are sequentially downregulated during recovery after immobilization-induced muscle atrophy. *Am J Physiol Endocrinol Metab* 2008; **295**: E1181–E1190.
- Charge SB, Rudnicki MA. Cellular and molecular regulation of muscle regeneration. *Physiol Rev* 2004; **84**: 209–238. doi:10.1152/physrev.00019.2003.
- Andrianjafinony T, Dupre-Aucouturier S, Letexier D, Couchoux H, Desplanches D. Oxidative stress, apoptosis, and proteolysis in skeletal muscle repair after unloading. *Am J Physiol Cell Physiol* 2010; **299**: C307–C315.
- Heng AE, Ventadour S, Jarzaguet M, Pouch-Pelissier MN, Guezennec CY, Bigard X, Attaix D, Taillandier D. Coordinate expression of the 19S regulatory complex and evidence for ubiquitin-dependent telethonin degradation in the unloaded soleus muscle. *Int J Biochem Cell Biol* 2008; **40**: 2544–2552.
- Taillandier D, Aourousseau E, Meynial-Denis D, Bechet D, Ferrara M, Cottin P, Ducastaing A, Bigard X, Guezennec CY, Schmid HP, Attaix D. Coordinate activation of lysosomal, Ca<sup>2+</sup>-activated and ATP-ubiquitin-dependent proteinases in the unweighted rat soleus muscle. *Biochem J* 1996; **316**: 65–72.
- Ogata T, Machida S, Oishi Y, Higuchi M, Muraoka I. Differential cell death regulation between adult-unloaded and aged rat soleus muscle. *Mech Ageing Dev* 2009; **130**: 328–336.
- Berthon P, Duguez S, Favier FB, Amirouche A, Feasson L, Vico L, Denis C, Freyssen D. Regulation of ubiquitin-proteasome system, caspase enzyme activities, and extracellular proteinases in rat soleus muscle in response to unloading. *Pflug Arch Eur J Physiol* 2007; **454**: 625–633.
- Gustafsson T, Osterlund T, Flanagan JN, von Walden F, Trappe TA, Linnehan RM, Tesch PA. Effects of 3 days unloading on molecular regulators of muscle size in humans. *J Appl Physiol* 2010; **109**: 721–727. doi:10.1152/jappphysiol.00110.2009.
- Reich KA, Chen YW, Thompson PD, Hoffman EP, Clarkson PM. Forty-eight hours of unloading and 24 h of reloading lead to changes in global gene expression patterns related to ubiquitination and oxidative stress in humans. *J Appl Physiol* 2010; **109**: 1404–1415.
- Gwag T, Lee K, Ju H, Shin H, Lee JW, Choi I. Stress and signaling responses of rat skeletal muscle to brief endurance exercise during hindlimb unloading: a catch-up process for atrophied muscle. *Cell Physiol Biochem* 2009; **24**: 537–546. doi:10.1159/000257510.
- Servais S, Letexier D, Favier R, Duchamp C, Desplanches D. Prevention of unloading-induced atrophy by vitamin E supplementation: links between oxidative stress and soleus muscle proteolysis? *Free Rad Biol Med* 2007; **42**: 627–635.
- Dupont-Versteegden EE. Apoptosis in skeletal muscle and its relevance to atrophy. *World J Gastroenterol* 2006; **12**: 7463–7466.
- Chen YW, Gregory CM, Scarborough MT, Shi R, Walter GA, Vandenborne K. Transcriptional pathways associated with skeletal muscle disuse atrophy in humans. *Physiol Gen* 2007; **31**: 510–520.
- Glover EI, Yasuda N, Tarnopolsky MA, Abadi A, Phillips SM. Little change in markers of protein breakdown and oxidative stress in humans in immobilization-induced skeletal muscle atrophy. *Appl Physiol Nutr Metab* 2010; **35**: 125–133.
- Baptista IL, Leal ML, Artioli GG, Aoki MS, Fiamoncini J, Turri AO, Curi R, Miyabara EH, Moriscot AS. Leucine attenuates skeletal muscle wasting via inhibition of ubiquitin ligases. *Muscle Nerve* 2010; **41**: 800–808.
- Vermaelen M, Sirvent P, Raynaud F, Astier C, Mercier J, Lacampagne A, Cazorla O. Differential localization of autolyzed calpains 1 and 2 in slow and fast skeletal muscles in the early phase of atrophy. *Am J Physiol Cell Physiol* 2007; **292**: C1723–C1731. doi:10.1152/ajpcell.00398.2006.
- Glass DJ. Skeletal muscle hypertrophy and atrophy signaling pathways. *Int J Biochem Cell Biol* 2005; **37**: 1974–1984.
- Krawiec BJ, Frost RA, Vary TC, Jefferson LS, Lang CH. Hindlimb casting decreases muscle mass in part by proteasome-dependent proteolysis but independent of protein synthesis. *Am J Physiol Endocrinol Metab* 2005; **289**: E969–E980.
- Nedergaard A, Jespersen JG, Pingel J, Christensen B, Sroczynski N, Langberg H, Kjaer M, Schjerling P. Effects of 2 weeks lower limb immobilization and two separate rehabilitation regimens on gastrocnemius muscle protein turnover signaling and normalization genes. *BMC Res Notes* 2012; **5**: 166. doi:10.1186/1756-0500-5-166.
- You JS, Park MN, Song W, Lee YS. Dietary fish oil alleviates soleus atrophy during immobilization in association with Akt signaling to p70S6k and E3 ubiquitin ligases in rats. *Appl Physiol Nutr Metab* 2010; **35**: 310–318. doi:10.1139/H10-022.
- Wickstrom SA, Lange A, Montanez E, Fassler R. The ILK/PINCH/parvin complex: the kinase is dead, long live the pseudokinase! *EMBO J* 2010; **29**: 281–291. doi:10.1038/emboj.2009.376.
- Hannigan GE, McDonald PC, Walsh MP, Dedhar S. Integrin-linked kinase: not so 'pseudo' after all. *Oncogene* 2011; **30**: 4375–4385. doi:10.1038/onc.2011.177.
- Carmignac V, Durbeej M. Cell-matrix interactions in muscle disease. *J Pathol* 2012; **226**: 200–218. doi:10.1002/path.3020.
- Miller MG, Naruszewicz I, Kumar AS, Ramlal T, Hannigan GE. Integrin-linked kinase is a positive mediator of L6 myoblast differentiation. *Biochem Biophys Res Commun* 2003; **310**: 796–803.
- Fukuda T, Chen K, Shi X, Wu C. PINCH-1 is an obligate partner of integrin-linked kinase (ILK) functioning in cell shape modulation, motility, and survival. *J Biol Chem* 2003; **278**: 51324–51333. doi:10.1074/jbc.M309122200.
- Shi Q, Bao S, Song L, Wu Q, Bigner DD, Hjelmeland AB, Rich JN. Targeting SPARC expression decreases glioma cellular survival and invasion associated with reduced activities of FAK and ILK kinases. *Oncogene* 2007; **26**: 4084–4094. doi:10.1038/sj.onc.1210181.
- Wang HV, Chang LW, Brixius K, Wickstrom SA, Montanez E, Thieversen I, Schwander M, Muller U, Bloch W, Mayer U, Fassler R. Integrin-linked kinase stabilizes myotendinous junctions and protects muscle from stress-induced damage. *J Cell Biol* 2008; **180**: 1037–1049. doi:10.1083/jcb.200707175.
- Riaz A, Zeller KS, Johansson S. Receptor-specific mechanisms regulate phosphorylation of AKT at Ser473: role of RICTOR in beta1 integrin-mediated cell survival. *PLoS One*. 2012; **7**: e32081. doi:10.1371/journal.pone.0032081.
- Nakamura K, Nakano S, Miyoshi T, Yamanouchi K, Nishihara M. Loss of SPARC in mouse skeletal muscle causes myofiber atrophy. *Muscle Nerve* 2013; **48**: 791–799. doi:10.1002/mus.23822.
- Weaver MS, Workman G, Sage EH. The copper binding domain of SPARC mediates cell survival *in vitro* via interaction with integrin beta1 and activation of integrin-linked kinase. *J Biol Chem* 2008; **283**: 22826–22837. doi:10.1074/jbc.M706563200.

35. Attaix D, Baracos VE. MAFbx/Atrogin-1 expression is a poor index of muscle proteolysis. *Curr Opin Clin Nutr Metab Care* 2010; **13**: 223–224. doi:10.1097/MCO.0b013e328338b9a6.
36. Bodine SC. Disuse-induced muscle wasting. *Int J Biochem Cell Biol* 2013; **45**: 2200–2208. doi:10.1016/j.biocel.2013.06.011.
37. Cho WJ, Kim EJ, Lee SJ, Kim HD, Shin HJ, Lim WK. Involvement of SPARC in *in vitro* differentiation of skeletal myoblasts. *Biochem Biophys Res Commun* 2000; **271**: 630–634. doi:10.1006/bbrc.2000.2682.
38. Petersson SJ, Jorgensen LH, Andersen DC, Norgaard RC, Jensen CH, Schroder HD. SPARC is up-regulated during skeletal muscle regeneration and inhibits myoblast differentiation. *Histol Histopathol* 2013; **28**: 1451–1460.
39. Nie J, Sage EH. SPARC inhibits adipogenesis by its enhancement of beta-catenin signaling. *J Biol Chem* 2009; **284**: 1279–1290. doi:10.1074/jbc.M808285200.
40. Cossu G, Borello U. Wnt signaling and the activation of myogenesis in mammals. *EMBO J* 1999; **18**: 6867–6872. doi:10.1093/emboj/18.24.6867.
41. Kim CH, Neiswender H, Baik EJ, Xiong WC, Mei L. Beta-catenin interacts with MyoD and regulates its transcription activity. *Mol Cell Biol* 2008; **28**: 2941–2951. doi:10.1128/MCB.01682-07.
42. Flint FO, Pickering K. Demonstration of collagen in meat products by an improved picro-Sirius red polarisation method. *Analyst* 1984; **109**: 1505–1506.
43. Livak KJ, Schmittgen TD. Analysis of relative gene expression data using real-time quantitative PCR and the 2<sup>−</sup>(Delta Delta C(T)) Method. *Methods* 2001; **25**: 402–408. doi:10.1006/meth.2001.1262.
44. Harridge SD, Andersen JL, Hartkopp A, Zhou S, Biering-Sorensen F, Sandri C, Kjaer M. Training by low-frequency stimulation of tibialis anterior in spinal cord-injured men. *Muscle Nerve* 2002; **25**: 685–694.
45. Carson JA, Booth FW. Myogenin mRNA is elevated during rapid, slow, and maintenance phases of stretch-induced hypertrophy in chicken slow-tonic muscle. *Pflugers Arch: Eur J Physiol* 1998; **435**: 850–858.
46. Yang H, Alnaqeeb M, Simpson H, Goldspink G. Changes in muscle fibre type, muscle mass and IGF-I gene expression in rabbit skeletal muscle subjected to stretch. *J Anat* 1997; **190**: 613–622.
47. Purslow PP. The structure and functional significance of variations in the connective tissue within muscle. *Comp Biochem Physiol* 2002; **133**: 947–966.
48. Kjaer M. Role of extracellular matrix in adaptation of tendon and skeletal muscle to mechanical loading. *Physiol Rev* 2004; **84**: 649–698. doi:10.1152/physrev.00031.2003.
49. Trotter JA, Purslow PP. Functional morphology of the endomysium in series fibered muscles. *J Morphol* 1992; **212**: 109–122. doi:10.1002/jmor.1052120203.
50. Zhao J, Brault JJ, Schild A, Cao P, Sandri M, Schiaffino S, Lecker SH, Goldberg AL. Foxo3 coordinately activates protein degradation by the autophagic/lysosomal and proteasomal pathways in atrophying muscle cells. *Cell Metab* 2007; **6**: 472–483.
51. Huang Y, Li J, Zhang Y, Wu C. The roles of integrin-linked kinase in the regulation of myogenic differentiation. *J Cell Biol* 2000; **150**: 861–872.